# Parallel ecological and evolutionary responses to selection in a natural bacterial community

Elze Hesse[1], Adela M. Luján[1, 2], Siobhan O'Brien[1, 3], Arthur Newbury[1], Terence McAvoy[1], Jesica Soria Pascual[1], Florian Bayer[1], Dave J. Hodgson[4] & Angus Buckling[1]

[1] CEC & ESI, Faculty of Environment, Science and Economy, University of Exeter, Penryn Campus, Cornwall, TR10 9FE, UK.

[2] Centro de Investigación y Desarrollo en Inmunología y Enfermedades Infecciosas (CIDIE), Consejo Nacional de Investigaciones Científicas y Técnicas (CONICET)/Universidad Católica de Córdoba (UCC), Córdoba, X5016DHK, Argentina. Facultad de Ciencias de la Salud, Universidad Católica de Córdoba (UCC), Córdoba, X5004ASK, Argentina.

[3] Current affiliation: Department of Microbiology, School of Genetics and Microbiology, Trinity College Dublin, College Green, Dublin 2, Ireland.

[4] CEC, Faculty of Environment, Science and Economy, University of Exeter, Penryn Campus, Cornwall, TR10 9FE, UK.

**Corresponding author |** Elze Hesse, CEC & ESI, Faculty of Environment, Science and Economy, University of Exeter, Penryn Campus, Cornwall, TR10 9FE, UK. Email: e.hesse@exeter.ac.uk.

**Key words |** bacteria, ecological species sorting, evolution, metal detoxification, public-goods, siderophores

**Abstract |** Evolution can occur over ecological timescales, suggesting a potentially important role for rapid evolution in shaping community trait distributions. However, evidence of concordant eco-evolutionary dynamics often comes from *in vitro* studies of highly simplified communities, and measures of ecological and evolutionary dynamics are rarely directly comparable. Here, we quantified how ecological species sorting and rapid evolution simultaneously shape community trait distributions by tracking within and between-species changes in a key trait in a complex bacterial community. We focused on the production of siderophores; bacteria use these costly secreted metabolites to scavenge poorly soluble iron and to detoxify environments polluted with toxic non-ferrous metals. We found that responses to copper-imposed selection within and between species were ultimately the same – intermediate siderophore levels were favored – and occurred over similar timescales. Despite being a social trait, this level of siderophore production was selected regardless of whether species evolved in isolation or in a community context. Our study suggests that evolutionary selection can play a pivotal role in shaping community trait distributions within natural, highly complex, bacterial communities. Furthermore, trait evolution may not always be qualitatively affected by interactions with other community members.

**Significance |** Bacterial communities possess remarkable taxonomic and metabolic diversity and play a key role in nearly every biogeochemical process on Earth. Rapid evolution (occurring over ecological time scales) can in principle shape these processes, yet we have little understanding of its importance in natural communities. Here, we quantified how the production of metal-detoxifying siderophores is driven by species compositional changes and evolution in a compost community in response to copper stress. We found that siderophore production converged at intermediate levels, with evolutionary

and ecological changes occurring at similar rates. Understanding how ecological and evolutionary processes contribute to shaping trait distributions will improve our ability to predict ecosystem responses to global change, and aid in the engineering of microbial consortia.

**Main text |** Changes in community trait distributions are typically driven by inter-specific competition changing the abundance of species carrying certain traits (i.e. ecological species sorting) (1). In the case of microbial communities, which have massive population sizes and short generation times, evolution can occur over timescales commensurate with ecological species sorting (2-4), suggesting a potentially important role of rapid evolution in shaping community trait distributions (5-7) and responses to environmental change (8). Understanding the mechanisms underpinning community trait distributions is not only of fundamental interest, but also has applied relevance (9-11), such as in the engineering of microbial consortia to perform valuable biological tasks (12), including bioremediation (13), and the development of microbiome technologies aimed at improving human health and crop yield (14).

Most work demonstrating a role of rapid evolution in community dynamics has been carried out in *in vitro* environments (2, 15) and/or has relied on the use of greatly simplified communities (3, 16, 17). This may overestimate the role of rapid evolution in community dynamics because, in addition to the typically very strong selection pressures associated with novel *in vitro* environments (4, 18), ecological complexity itself can constrain evolution (19-22) (but see (23)). The response to selection – resulting from ecological species sorting or within-species evolutionary change – typically increases with trait variation (24). Increasing species diversity can both increase between-species trait variation and reduce within-species variation – the latter because of reduced population

sizes (25, 26). The relative importance of ecological species sorting versus evolution on shaping trait distributions is therefore likely to increase with species diversity (1, 19). While some recent work has demonstrated rapid evolution occurring over ecological timescales in more complex communities and/or semi-natural environmental contexts (2-4), the role of ecological species sorting versus evolutionary selection in shaping natural community trait distributions is unclear.

A useful model system to track simultaneous ecological and evolutionary changes in functional traits is the ubiquitous production of metal-chelating siderophores in bacterial communities (27). Although perhaps best known for their function as iron carriers (28, 29), siderophores can also protect bacteria from toxic metal stress by preventing the diffusion of toxic metals into bacterial cells (30, 31). Because detoxification takes place in a shared environment, these costly extracellular compounds not only protect the producer, but potentially also neighboring conspecifics (32) and other community members (33, 34). By acting as community-wide public-goods, siderophores play a key role in driving species interactions (35) and adaptive responses to environmental change (34). We previously determined the effect of toxic metals on siderophore production in natural bacterial communities inhabiting mine-degraded soils (33, 36) as well as in experimental compost communities exposed to copper stress (33). In both cases, the presence of toxic metals selectively favored bacterial taxa with greater investment in siderophores, thereby increasing community-wide siderophore levels. However, we have also found that bacterial taxa can benefit from siderophores produced by conspecifics (32) or individuals from phylogenetically diverse taxa (34), suggesting that selection for (higher or lower) siderophore production may also be affected by social interactions.

Here, we investigate ecological changes in siderophore production in response to copper stress in a compost bacterial community simultaneously with evolutionary change in siderophore production by a focal bacterium – the common soil-dwelling bacterium

104 *Pseudomonas fluorescens* (strain SBW25) (37). We hypothesized that ecological changes
105 in siderophore production resulting from exposure to novel copper stress would be greater
106 than evolutionary changes that occurred within SBW25. We also expected the community
107 to alter the evolutionary trajectory of SBW25's siderophore production as a consequence
108 of both community-imposed evolutionary constraints and greater selection for lower-level
109 siderophore production resulting from the protective effects afforded by other community
110 members.
111

112 ## Results

113 ### Copper favors siderophore-producing taxa within the compost community

114 We set up a fully factorial experiment involving the presence/absence of the natural
115 compost community, focal strain *Pseudomonas fluorescens* SBW25 and copper pollution
116 in initially sterile compost (SI Appendix, Fig. S1). These communities were allowed to
117 evolve for six weeks, after which we quantified changes in siderophore production by
118 isolating 24 clones of SBW25 and 24 isolates per replicate community where possible (i.e.
119 $n = 48$ isolates for the SBW25 + community treatments). Isolates were then grown
120 individually in King's B medium for 48 hrs after which we measured the ability of culture
121 supernatants to chelate iron using colorific CAS assays, corrected for variation in optical
122 density (our measure of siderophore production is based on arbitrary unity; see Methods).
123 We found that copper selected for greater siderophore levels within the compost
124 community compared to unpolluted control communities (Fig. 1A), irrespective of the
125 presence of SBW25 (2-way GLM on mean community siderophore production: $F_{1, 20} =$
126 $0.01$, $P = 0.91$ for copper × SBW25, $F_{1, 21} = 0.04$, $P = 0.85$ for SBW25 and $F_{1, 22} = 8.88$, $P$
127 $< 0.01$ for copper treatment. GLM estimates of mean siderophore production ± 95%
128 confidence intervals [CI] in copper-polluted versus unpolluted communities pooled across

129 SBW25 levels (i.e. presence/absence): 0.55 [0.53, 0.57] and 0.50 [0.48, 0.52],
130 respectively).
131 To determine whether the observed shifts in siderophore production were linked to
132 any compositional changes in the community, we determined the genus-level identity of all
133 final-time-point compost isolates assayed for siderophore production ($n$ = 548 isolates in
134 total). We found that copper-mediated changes in siderophore production were
135 accompanied by a shift in community composition (2-way PERMANOVA on Bray–Curtis
136 dissimilarities: copper × social context: $F_{1, 20} = 2.47$, $P = 0.03$), with between-community
137 diversity differing significantly across all treatment combinations (pairwise
138 PERMANOVAs: $R^2 > 0.26$, all $P_{adj} < 0.05$; Fig. 1B). In particular, the presence of SBW25
139 changed the relative abundance of taxa within the compost community by suppressing
140 *Pseudomonas, Bacillus* and *Arthrobacter* compared to the community-only treatment (all
141 $P_{adj} < 0.05$; SI Appendix, Fig. S2). We also found that copper tended to select against taxa
142 that displayed relatively low mean levels siderophore production (i.e. blue taxa in Fig. 1C):
143 in particular, while intermediate siderophore producers, such as *Cupriavidus*, were
144 significantly more abundant in copper-polluted communities, *Achromobacter* and
145 *Lysinibacillus* were negatively affected by copper stress (SI Appendix, Table S1). As a
146 result of such ecological species sorting, the most abundant community members in
147 copper-polluted compost were those displaying more intermediate siderophore levels (Fig
148 1D). Note that evolution may also have contributed to changes in siderophore production,
149 but this is impossible to quantify from these taxonomic results. We therefore focus on
150 evolution within a focal strain.
151

152 **Copper selects against high siderophore levels within SBW25**

153 We tracked siderophore changes within replicate populations of SBW25 that had either
154 evolved in the presence or absence of the compost community. We found the exact

155 opposite response compared to that observed at the community level – toxic copper
156 selectively favored SBW25 individuals that, on average, produced lower amounts of
157 siderophore compared to control populations (LMM: copper effect: $\chi^2_1$= 10.97, $P < 0.001$.
158 Mean siderophore production ± 95% CI in copper-polluted versus control populations:
159 0.68 [0.67, 0.70] and 0.72 [0.71, 0.73], respectively). Again, the impact of copper stress on
160 siderophore production did not differ significantly as a function of community
161 presence/absence (LMM: interaction between copper × community: $\chi^2_1$= 0.22, $P = 0.64$;
162 community effect: $\chi^2_1$= 1.97, $P = 0.16$; Fig. 2).
163
164 **Copper selects against siderophore extremes**
165 How can we resolve these apparently opposing responses to copper-imposed selection
166 operating at the species versus community level? To answer this question, we first
167 compared the shape of the distribution of siderophore production of the compost
168 community to that of SBW25. We found that copper selected against siderophore
169 extremes, resulting in trait convergence (Fig. 3), regardless of whether SBW25 and the
170 community were grown in isolation or together in co-culture.
171 To quantify this convergence, we focused on the effect that copper has on
172 siderophore production when the community and SBW25 were grown together, using a
173 hierarchical Bayesian linear model to account for heteroscedasticity between isolate types
174 (community versus SBW25; all point estimates are *maximum a posteriori estimates* ± 95%
175 credible intervals). The copper-mediated change in siderophore production in SBW25 was
176 -0.042 [-0.072, -0.014]. In contrast, copper stress increased siderophore production among
177 compost community isolates by 0.044 [0.009, 0.081]. Thus, the effect was of
178 approximately equal magnitude, but in the opposite direction. Indeed, combining the
179 posterior estimates for the effect of copper on siderophore production in SBW25 and in the

180 rest of the community (positive values indicate that the positive effect on community
181 isolates is larger than the negative effect in SBW25 and *vice versa*), the estimated
182 combined effect was 0.001 [-0.044, 0.045]. In the absence of copper, the difference in
183 siderophore production between SBW25 and the compost community was 0.216 [0.185,
184 0.251]. Copper pollution significantly reduced this figure by 0.086 [0.041, 0.133] to 0.130
185 [0.098, 0.161]. Thus, opposing and approximately equal effects of selection lead to a
186 significant reduction in the difference between (relatively high producing) SBW25 and
187 (relatively low producing) community isolates under copper stress.

188 The model described above included separate standard deviation parameters for
189 each sample type (community/SBW25 × copper/no copper) to estimate their respective
190 within-microcosm variation in siderophore production. The standard deviation of
191 siderophore production amongst SBW25 isolates was 0.0294 [0.0267, 0.0340] in the
192 absence of copper. The copper treatment led to an increase of 0.006 [-0.00031, 0.0131] to
193 0.0354 [0.0315, 0.0427]. Conversely, variation in siderophore production was reduced
194 amongst compost community isolates in the presence of copper. Here, the standard
195 deviation fell from 0.0994 [0.0899, 0.115] to 0.0693 [0.0633, 0.0808] in response to the
196 copper treatment, a significant difference of 0.0301 [0.0157, 0.0474]. That the overall
197 variation in siderophore production was much higher in the compost community than
198 SBW25 is expected, since measurements were taken from a range of unrelated strains. The
199 decrease in variance due to copper stress suggests ecological species sorting (and some
200 evolutionary change), whereas the increase in variance within SBW25 isolates is
201 compatible with evolutionary change.

202 To further investigate the generality of this result, we focused on isolates of
203 representative genera ($n$ = 8 genera) that occurred in both copper environments and had
204 been assayed for siderophore production. We found that trait changes were qualitatively
205 similar: copper selected against siderophore extremes. That is, taxa with high 'baseline'

206 siderophore levels (i.e. mean siderophore levels > 0.55 in control conditions) produced
207 fewer siderophores in copper-polluted compost (Cohen's $d < 0$; SI Appendix, Fig. S3). In
208 contrast, copper stress favored greater siderophore production in bacterial taxa with low
209 'baseline' siderophore levels (Cohen's $d > 0$). Hence, we found a negative relationship
210 between effect size and 'baseline' siderophore levels (Spearman rank correlation: $S =$
211 $624.36$, $P = 0.005$, $\rho = -0.72$).
212
213 **Direct fitness costs of high levels of siderophore production in copper**
214 Selection for siderophore production in the presence of toxic copper can be explained by
215 the direct protective effects afforded by siderophores. However, what is less clear is why
216 there was selection against *high* levels of siderophore production in toxic copper
217 conditions. There are two general, non-mutually exclusive explanations. First, there may
218 be a direct cost associated with greater investment in siderophores in copper when
219 individuals produce more than enough siderophore to detoxify copper, making the excess
220 an unnecessary metabolic burden. Second, individuals producing high levels of
221 siderophore may protect competing conspecific and heterospecific individuals, increasing
222 the relative cost of siderophore production.
223 We first explored how evolved changes in siderophore production affect individual
224 performance in toxic copper conditions. Specifically, we determined whether SBW25
225 clones that had evolved to produce relatively low levels of siderophore displayed lower
226 copper tolerance ($n = 277$ clones in total, all isolated from the 'no community' treatment;
227 SI Appendix, Fig S1). To this end, evolved clones were individually grown in King's B
228 broth supplemented with a toxic dose of copper sulphate (final concentration of 6.17 mM
229 $CuSO_4$). We recorded changes in optical density ($OD_{600}$) over a 48-hrs period and
230 estimated clone-specific Malthusian growth parameters ($m$). Our results show that clones
231 that had evolved in copper-free and copper-polluted compost grew equally well in toxic

232 copper broth (LMM: effect of evolutionary background on *m*: $\chi^2_1$= 0.76, *P* = 0.39; SI
233 Appendix, Fig. S4), suggesting that siderophores are effective in detoxifying copper.
234 Furthermore, reduced investment in siderophores did not confer lower tolerance,
235 irrespective of a clones' evolutionary history (LMM on *m*: siderophore production ×
236 copper background: $\chi^2_1$= 0.02, *P* = 0.88; copper background: $\chi^2_1$= 0.16, *P* = 0.69;
237 siderophore production: $\chi^2_1$= 2.95, *P* = 0.09; SI Appendix, Fig. S4). The observed shift
238 towards reduced siderophore levels in SWB25 therefore did not alter copper tolerance.
239 We next investigated why high investment in siderophores is costly in the presence
240 of copper but not in the absence. We speculated that the constrained growth of SBW25 in
241 the presence of copper (SI Appendix, Fig. S5) may have reduced levels of siderophore
242 required for the canonical function of siderophores: iron uptake (38). To test this
243 hypothesis, we manipulated population growth rates (and hence indirectly the need for iron
244 to sustain growth) by inoculating monocultures of the wild-type pyoverdine-producing
245 SBW25 strain and an isogenic pyoverdine-deficient mutant (PBR840) (39) in sterile
246 compost at very low density (allowing for faster growth) and high density (allowing for
247 slower growth), both in the presence and absence of copper pollution. This mutant does not
248 produce the main siderophore pyoverdine (which reduces total siderophore production to
249 21% of the wild- type) and displays levels of siderophore production similar to an average
250 compost community member.
251 Confirming our observations on copper tolerance in evolved SBW25 populations,
252 the pyoverdine-deficient mutant performed equally well compared to the pyoverdine
253 producing strain in copper-polluted compost (GLM on *m*: copper × strain: $F_{1,43}$ = 0.52, *P* =
254 0.48; Fig. 4A), with copper significantly reducing population growth (main effect copper:
255 $F_{1,44}$ = 100.24, *P* < 0.001. Mean growth ± 95% CI: $\overline{m}_{control}$ = 1.50 [1.45, 1.55] and
256 $\overline{m}_{copper}$1.14 [1.09, 1.19], pairwise contrast: *t* ratio = 10.01, *P* < 0.001), irrespective of

257 inoculation density (copper × density: $F_{1,40}$ = 0.22, $P$ = 0.65). We also found that in both
258 copper environments, the pyoverdine producers benefitted when inoculated at low density
259 and hence growth was not constrained (strain × density: $F_{1,43}$ = 16.30, $P$ < 0.001;
260 $\bar{m}_{producer}$ = 1.98 [1.90, 2.05] and $\bar{m}_{deficient}$ 1.88 [1.81, 1.95], pairwise contrast: $t$ ratio =
261 1.89, $P$ = 0.07; Fig. 4A). In contrast, the non-producing mutant grew faster than the
262 producer under slow (high inoculation density) growth conditions ($\bar{m}_{producer}$ = 0.61 [0.54,
263 0.69] and $\bar{m}_{deficient}$ = 0.81 [0.74, 0.88], pairwise contrast: $t$ ratio = -3.82, $P$ <0.001).
264 Consistent with this monoculture pattern, the relative fitness of the pyoverdine producer
265 was greater when competing with the mutant under high growth conditions (low
266 inoculation density), while it was lowest under low growth conditions (GLM on $r_{producer}$:
267 density × copper interaction: $F_{1,19}$ = 6.95, $P$ = 0.016) – especially in the presence of copper
268 (high density: $\bar{r}_{copper}$ = 0.79 [0.73, 0.85 ]and $\bar{r}_{control}$ = 0.91 [0.85, 0.97], pairwise contrast:
269 $t$ ratio = 2.92, $P$ < 0.01 and low density: $\bar{r}_{copper}$ = 1.04 [0.98, 1.10] and $\bar{r}_{control}$ = 1.00
270 [0.94, 1.07], pairwise contrast: $t$ ratio = -0.86, $P$ = 0.40. Data on Malthusian growth and
271 relative fitness are presented in SI Appendix, Fig. S6). These results suggest a cost to high
272 investment in siderophores when growth is otherwise constrained, while there is no cost
273 and potentially a benefit to high levels of siderophore production when growth is less
274 constrained, and these compounds are needed to compete for iron.
275
276 **Public-goods exploitation favors reduced investment in siderophores**
277 While direct costs and benefits could qualitatively explain our results, we next
278 explored whether public-goods exploitation could have played an additional role in driving
279 selection against SBW25 individuals producing relatively large amounts of siderophores.
280 Previous work investigating within-species exploitation of siderophores has demonstrated
281 that siderophore production is costly to the individual (40, 41), creating incentives for non-

282 producing ‘cheats’ to invade and steal these public-goods away from the producer (42).
283 We have also found that bacterial compost isolates that invest relatively little in
284 siderophores benefit from other species’ detoxifying siderophores under similar levels of
285 copper stress (34). However, siderophore-mediated facilitation could not fully rescue the
286 growth of copper-sensitive isolates, nor did it result in exploitation (i.e. no detectable
287 indirect costs by helping competitors) within the community over ecological timescales
288 (34). Combined with our current finding of parallel changes in siderophore distribution at
289 the within-taxon and community level (Fig. 3), we focus on social dynamics *within* species
290 only.

291 To determine whether individuals with lower siderophore investment can exploit
292 relatively high producers we carried out competition assays. In particular, we manipulated
293 the relative frequencies of the wildtype and pyoverdine-deficient mutant of SBW25 (1% or
294 99% starting frequency of strains) and assayed their relative performance following 7 days
295 of growth in copper-polluted and unpolluted compost. Negative frequency-dependent
296 fitness often characterizes social interactions in structured environments, where rare non-
297 producing ‘cheats’ are more likely to readily encounter cooperators rather than other cheats
298 and grow relatively well, while rare cooperators will mostly encounter cheats, but so will
299 other cheats; with the latter suffering a greater relative growth cost. We found that the
300 pyoverdine-deficient mutant experienced a relative selective benefit when rare, in
301 particular in toxic copper conditions (GLM on selection coefficient (*s*) of pyoverdine-
302 deficient mutant: frequency × copper: $F_{1, 44} = 79.30$, $P < 0.001$. Mean ± [95% CI] for
303 control: $s_{high} = 0.045$ [-0.08, 0.13] and $s_{low} = 0.33$ [0.25, 0.41]; pairwise contrast; *t* ratio =
304 -4.95, $P < 0.001$. Mean ± [95% CI] for copper: $s_{high} = 0.301$ [0.22, 0.38] and $s_{low} = 1.31$
305 [1.22, 1.39]; pairwise contrast; *t* ratio = -17.55, P < 0.001; Fig. 4B. Data on Malthusian
306 growth are presented in SI Appendix, Fig. S7). This shows that in addition to direct fitness

307 effects, social exploitation by conspecifics could also have contributed to the evolution of
308 reduced siderophore production by SBW25 in response to copper stress.
309

310 **Discussion**

311 Using siderophores as a focal trait, we show that evolutionary and ecological processes
312 operate in parallel and over similar timescales in a natural bacterial community, resulting
313 in trait convergence towards intermediate siderophore levels in response to copper stress.
314 In particular, copper-imposed selection changed the relative abundance of bacterial taxa by
315 selecting against individuals that displayed extremes in siderophore investment. This
316 pattern was consistent at the community- and within-taxon level. Crucially, changes in
317 siderophore production not only resulted from ecological species sorting, but also from
318 evolutionary changes within species: SBW25 adapted to copper stress by lowering its
319 investment in siderophores to levels more comparable to that of an average compost
320 community member.

321 In our system, copper pollution resulted in selection against siderophore extremes.
322 We propose such stabilizing selection in part resulted from directly incurred costs borne by
323 taxa with relatively low and high siderophore production. In particular, we have previously
324 shown that bacterial compost taxa that invest relatively little in siderophores display
325 reduced copper tolerance and suffer an absolute growth cost (34). Our current findings
326 indicate that beyond a certain threshold, increased investment in detoxifying siderophores
327 resulted in diminishing returns, thereby selecting against individuals producing relatively
328 large amounts of siderophore.

329 This raises the question as to why siderophore production was maintained at higher
330 levels in unpolluted compared to copper-polluted environments. It has been well-
331 established that siderophores play an important role in scavenging insoluble iron from the

environment (43). Ironbound siderophores are typically imported by specific receptors that constrain their use by other competing strains, thereby limiting siderophore cross-feeding between strains (but see (44, 45)). As such, siderophores are thought to play a key role in determining the outcome of interspecific competition for iron (46, 47). Hence, siderophores were likely positively selected for in copper-free conditions to pillage iron from competing strains. By contrast, competition for iron was likely reduced under copper stress because iron no longer limited bacterial growth rates (copper did); the main role of siderophores in copper-polluted conditions was to detoxify metals.

Social conflict and cooperation are often thought to play a key role in driving the eco-evolutionary dynamics of microbial communities (48-53). In microbes, social behaviors are often mediated by secretion of 'public-goods' – metabolically costly compounds that benefit the producer, but that are open to exploitation by non-producers that do not contribute their fair share but utilize the benefits afforded by their production (54). Most of our understanding of public-good dynamics comes from work on within-species interactions (55), yet many public-goods can simultaneously benefit other species (56-60), particularly in microbial communities. Key examples include antibiotic-degrading enzymes (61, 62), resource-scavenging molecules (55, 63), immune-manipulating effectors (64-67) and potentially siderophore-mediated detoxification. However, we found little evidence to suggest that inter-specific facilitation and exploitation shaped siderophore production in this experiment: siderophore production of neither the community nor SBW25 was qualitatively affected by the other, despite – and in line with previous work – SBW25 greatly altering community composition over the course of our experiment (68). We did find some evidence for within-species exploitation: the pyoverdine-deficient 'cheat' accrued a relative fitness benefit when competing with wild-type pyoverdine-producing SBW25, in particular when rare, both in the presence and absence of copper. Such frequency dependent dynamics are indicative of intraspecific exploitation of public-

358 goods in spatially structured environments (55, 69-71), and is predicted to increase
359 variation within species while decreasing divergence between species, which is borne out
360 by our results.

361 In our experiment we quantified the *potential* of bacterial isolates to produce
362 siderophores rather than their *in-situ* production in compost. The transcription of genes
363 encoding the proteins that participate in siderophore biosynthesis is tightly regulated by the
364 presence of iron and/or toxic metals (30). However, the use of a common garden
365 environment to quantify siderophores was necessary because: (1) for the majority of
366 environmental isolates we do not exactly know what kind of metal-chelating agents they
367 produce, meaning a metagenomics approach is currently not viable; (2) it is notoriously
368 difficult to extract siderophores from soil and link their production to specific taxa and (3)
369 the presence of soil organic material and other factors in compost interferes with CAS
370 assays. Notwithstanding, we demonstrate a direct link between relative changes in
371 siderophore potential and fitness.

372 Our focus on public-goods traits, such as siderophore production, may have over-
373 estimated the role of evolution. Previous work has shown that public-goods cheats readily
374 emerge via loss-of-function mutations, including cheats defective for quorum sensing (72)
375 or the production of extracellular proteases (73), polysaccharides (74) and siderophores
376 (70). For example, pyoverdine-deficient cheats typically evolve within days in the lab (75),
377 often via single SNPs in regulatory genes. However, over-estimation of the role of
378 evolution may be mitigated to some extent because, compared to many studies on the
379 evolution of public-goods, we evolved compost communities over an extended period
380 which also allowed for major shifts in community composition. More broadly, adaptive
381 evolution of a wide range of non-social traits can result from loss-of-function mutations
382 through rewiring of regulatory and metabolic networks (76). Finally, gain of functions,
383 including potential public-goods traits, can also potentially evolve very rapidly via

384 horizontal gene transfer (HGT; 77, 78, 79) (80). HGT can occur across large phylogenetic
385 distances (81), which could actually increase the relative importance of evolution *versus*
386 species sorting in shaping community trait distributions.

387 To conclude, we show that the importance of rapid evolution in shaping community
388 trait distributions is not limited to simplified *in vitro* communities but can also play a role
389 as important as species sorting within highly complex natural microbial communities.
390 Furthermore, our results suggest that trait evolution may not always be qualitatively
391 affected by interactions with other community members.

392

## 393 Methods

394 All supporting data and R code are available at https://zenodo.org/records/11639136.
395 Sequences have been deposited at ENA Project PRJEB29924:
396 https://www.ebi.ac.uk/ena/data/search?query=PRJEB29924.

397

### 398 Bacterial strains

399 We used *Pseudomonas fluorescens* strain SBW25 as our focal species (37). This common
400 soil-dwelling bacterium produces a variety of siderophores, including pyoverdine (45) and
401 an ornicorrugatin-like siderophore (82), that are able to chelate iron. The strain's primary
402 siderophore – pyoverdine – has been shown to bind copper (30), which renders the
403 environment less toxic by preventing diffusion into the bacterial cell (31). To facilitate
404 isolation of SBW25 from the community, the strain was modified by inserting a LacZ
405 genetic marker and a gentamicin-resistance cassette, which resulted in blue resistant
406 colonies when plated out on Lysogeny Broth (LB) agar supplemented with 90μg/mL 5-
407 Bromo-4-chloro-3-indolyl-β-D-galactopyranoside (X-gal) and 25 μg/mL gentamicin (32).

408 To isolate the compost community, 40 gr of fresh compost (Verve John Innes No.
409 1) was added to 200 mL of M9 minimal salt solution and incubated shaken at 150 rpm at
410 28 °C for 24h. The supernatant was plated out on LB agar to verify the presence of a
411 bacterial community, and also on LB supplemented with 30µg/mL gentamicin to verify the
412 susceptibility of the community to this antibiotic (32). A 20% glycerol stock solution was
413 prepared from the aqueous sample suspension and frozen at -80°C for future use.
414

415 **Selection experiment**

416 Compost microcosms were established with 30 gr of twice-autoclaved sterile compost in
417 round 90 mm petri dishes. To track ecological and evolutionary changes in siderophore
418 production, we seeded twelve replicate compost microcosms with (1) a soil wash of the
419 isolated compost community, (2) an overnight culture of SBW25 or (3) both together at a
420 1:1 ratio ($n$ = 36 compost microcosms in total, SI Appendix, Fig. S1), keeping total
421 inoculation density constant (~$5 \times 10^7$ cells). Note that results of the community-only
422 treatment were published previously (33). Compost microcosms were incubated at 26°C
423 and 75% relative humidity for 24h, after which half of the microcosms of the above
424 treatments ($n$ = 6) was supplemented with a toxic dose of copper (2 mL of filter-sterilized
425 0.25M $CuSO_4$) and the remainder with an equal volume of sterile *dd*$H_20$ (33). Microcosms
426 were incubated for a total of 6 weeks. After three weeks, a second dose of copper or
427 *dd*$H_2O$ was added to the relevant microcosms. Samples were taken just before ('ancestral')
428 and 6 weeks after copper amendment ('evolved') by transferring 1 gr of compost per
429 microcosm to 6 mL of M9 solution in 30 mL glass vials. Vials were shaken for 2h at 26°C
430 at 180 rpm, after which supernatants were frozen in glycerol (25% final concentration) at -
431 80°C for future assays.
432

433 **Phenotypic assays on ancestral and evolved isolates**

434 *Siderophore production*

435 To quantify siderophore production, serial-diluted freezer stocks (taken just before and 6
436 weeks after giving the first dose of copper) were plated out on duplicate LB agar plates
437 supplemented with (i) X-gal to isolate members of the compost community or (ii) X-gal
438 and gentamicin to isolate SBW25 colonies. Following 48 hours of incubation at 26°C,
439 individual colonies could be identified, counted and picked. For each unique treatment-
440 time combination, we picked 24 colonies of the compost community and/or SBW25 per
441 replicate, with a total of 48 colonies picked from compost microcosms seeded with both
442 SBW25 and the community. Individual colonies were grown in KB broth for 48h at 26°C,
443 after which the supernatant was assayed for the extent of iron chelation. Siderophore
444 production was quantified using the liquid CAS assay described by Schwyn and Neilands
445 (83). Siderophore production per isolate was estimated using: $[1 - (A_i/A_{ref})] /(OD_i)$, where
446 $OD_i$ = optical density at 600 nanometer (nm) and $A_i$ = absorbance at 630 nm of the assay
447 mixture and $A_{ref}$ = absorbance at 630 nm of reference mixture (KB+CAS; $A_{ref}$). For some
448 samples, absorbance reads were negative following reference correction, so we
449 standardized siderophore production by setting the minimum observed value to zero. Note
450 that CAS assays performed in iron-limited KB medium provided qualitatively similar
451 results (34).

452

453 *Copper tolerance*

454 We determined the direct fitness consequences of copper-imposed reductions in
455 siderophore production in SBW25. Final-time-point clones ($n$ = 277) isolated from
456 populations that had evolved in the absence of the community were grown individually at
457 26°C for 24h, after which ~ $10^4$ cells were inoculated into 96-well plate wells containing
458 200 μL of King's B broth supplemented with a toxic dose of copper sulphate (final
459 concentration of 6.17 mM $CuSO_4$). Individual clones were incubated statically at 26°C for

460 52 hours, and their optical densities ($OD_{600}$) were measured every 8–12 h (Varioskan Flash
461 plate reader, Thermo Scientific, Waltham, MA, USA). We determined the Malthusian
462 growth parameter (*m*) for each clone as: ln(final density / start density) / time (hours) (84).
463

464 **Sanger sequencing of compost isolates**

465 The 16S rRNA gene of all final-time-point compost isolates assayed for siderophore
466 production was sequenced to confirm genus-level identity (i.e. $n = 24$ per replicate). PCRs
467 were performed in 25µL reactions containing 1x DreamTaq Green PCR Master Mix (2X)
468 (Thermo Scientific), 200 nM of the 27F and 1492R primers and 3 µL of 1:100 diluted
469 culture that had undergone 3 freeze-thaw cycles. The thermal cycling parameters were set
470 to 94ºC for 4 min, followed by 35 cycles of 1 min at 94ºC, 30s at 48ºC and 2 min at 72ºC,
471 and a final extension of 8 min at 72ºC. Following Exo-AP clean-up, high quality samples
472 were Sanger sequenced using the 27F primer (Core Genomic Facility, University of
473 Sheffield). Sequence quality was assessed using the R 'dada2' package (85), and
474 sequences were trimmed in Genious (86) to achieve an overall quality score >35. Using
475 Mothur (87), sequences longer then 300bp were then aligned to the Silva.Bacteria.Fasta
476 database, and taxonomy was classified using the RDP trainset 14 032015 as a reference
477 database.
478

479 **The role of siderophores as iron-scavengers as a function of density**

480 To determine whether high siderophore production was selected against as a result of iron
481 being less limited under toxic copper conditions, we conducted competition assays
482 between the pyoverdine-producing LacZ-marked SBW25 strain (37) and an isogenic
483 pyoverdine-deficient mutant (PBR840) (39) in 30 mL glass universals containing 5 grams
484 of twice-autoclaved sterile compost. Using a full-factorial design, strains were grown in
485 isolation or together at a 1:1 ratio at either low ($10^2$ CFUs) or high inoculation density ($10^6$

486 CFUs), keeping total inoculation density constant across these social contexts. Compost
487 microcosms were incubated for 24 hours at 26°C and 75% relative humidity, after which
488 we added a toxic dose of $CuSO_4$ (1 mL of 0.25M $CuSO_4$) to half of the microcosms and an
489 equal volume of sterile *dd*$H_2O$ to the remainder *(n* = 6 replicates per treatment). Compost
490 microcosms were incubated for a total of 7 days, after which soil washes were taken, serial
491 dilutions of which were plated out on KB agar. For co-cultures, strains could be
492 distinguished based on their colony pigmentation: wild-type colonies were blue on X-gal
493 supplemented KB agar, whereas mutant colonies were white. We determined the
494 Malthusian growth parameter (*m*) for each strain as described above.
495

496 **Public-goods exploitation in SBW25**

497 To determine whether social exploitation could have played an additional role in driving
498 copper-mediated reductions in siderophore production in SBW25, we conducted
499 competition assays between the pyoverdine-producing wild-type and pyoverdine-deficient
500 mutant strain of SBW25 in petri dishes containing 30 gr of twice-autoclaved sterile
501 compost. Using a full-factorial design, strains were inoculated together at a low (1%, $10^4$
502 CFUs, *n* = 24) or high (99% $10^6$ CFUs, *n* = 24) frequency. Compost microcosms were
503 incubated for 24 hours at 26°C and 75% relative humidity, after which we added a toxic
504 dose of $CuSO_4$ (2 mL of 0.25M $CuSO_4$) to half of the microcosms and an equal volume of
505 sterile *dd*$H_2O$ to the remainder. Following 7 days of incubation, soil washes were taken
506 and plated out on KB agar supplemented with X-gal to distinguish between strains. We
507 determined the Malthusian growth parameter (*m*) for each strain as above.
508

509 **Data analyses**

510 For all analyses, we used *R* Version 4.0.3 (R Development Core Team; http://www.r-
511 project.org). In general, models were compared by sequentially deleting terms and
512 comparing model fits using F-tests or $\chi^2$-tests (where appropriate), after which pairwise
513 contrasts were computed using the 'emmeans' packages (88), with $\alpha < 0.05$. In case of
514 multiple pairwise testing, *P*-values were adjusted using the false discover rate ('fdr')
515 method unless stated otherwise. We checked residual behaviour using the 'DHARMa'
516 package (89). All plots were produced using the 'ggplot2' package (90).
517
518 *The effect of copper on community structure and mean levels of siderophore production*
519 To test for the effect of copper on siderophore production in compost communities that had
520 either evolved with or without SBW25, we initially used a linear mixed effects (LMM)
521 model (*'lmer'* function in *'lme4'* package) (91) with copper × SBW25 presence as fixed
522 explanatory variables, as well as their interaction. To account for non-independency of
523 observations we fitted random intercepts for individual microcosms. However, we
524 observed strong heteroscedasticity of residuals, which could not be remedied by including
525 a treatment-specific variance structure. For each replicate community, we therefore
526 averaged siderophore production across the 24 compost isolates assayed and used a 2-way
527 generalized linear model (GLM) with a Gaussian error distribution to test for the
528 interactive effect of copper × SBW25 presence on mean community-wide siderophore
529 production. This simplified model gave qualitatively very similar results to the LMM
530 without violating any underlying model assumptions.
531 We determined the genus-levels identity of all end-point compost isolates assayed
532 for siderophore production ($n$ = 24 per community) and used PCoA ordination plots to
533 depict pair-wise Bray-Curtis dissimilarities in community composition between
534 microcosms (excluding observations on SBW25). To test for the interactive effect of
535 copper × SBW25 presence on community structure we ran a permutational 2-way

536 ANOVA test on Bray-Curtis dissimilarities using the '*adonis2*' function in the '*vegan*'
537 package (92) with 9999 permutations. Following this, we ran pairwise permutational
538 ANOVAs to disentangle which treatments differed significantly from one another using
539 the *'calc_pairwise_permanovas'* function in the '*mctoolsr'* package
540 (https://github.com/leffj/mctoolsr/), with *P*-values corrected for multiple testing using the
541 'fdr' method. We confirmed homogeneity of variance using the *'betadisper'* function in
542 the '*vegan'* package to estimate group differences in dispersion and treated all copper ×
543 SBW25 combinations as levels of a single factor in a 1-way AVOVA on dispersion.
544 To determine which of the compost isolates differed in abundance across
545 treatments, we fitted a negative binomial GLM to the data using the '*DESeq'* function in
546 the R package '*DESeq2*' (93). We focused on a subset of ten common compost isolates
547 that occurred in both unpolluted and copper-polluted communities. Based on the outcome
548 of pairwise permutational ANOVAs (see above), we initially included the interaction term
549 between copper × SBW25 presence in the design of our GLM. However, following model
550 reduction (LRT tests), the minimal adequate model was best described by only including
551 the additive effect of copper and community context. Using this additive model, we
552 calculated significant differences in the abundance of taxa using Wald tests and we
553 corrected *P* –values for multiple testing for each of two contrasts used (presence/absence
554 of either SBW25 or copper).
555
556 *The effect of copper on mean siderophore production in a focal strain*
557 To test for the interactive effect of copper and community context on siderophore
558 production in SBW25, we used a LMM model with copper × community presence as fixed
559 explanatory variables, as well as their interaction. To account for non-independency of
560 observations, we fitted random intercepts for individual microcosms. Based on the
561 obtained simulation-based residual plots, we included a dispersion parameter for each of

562 the copper × community levels, using the *'glmmTMB'* function in the *'glmmTMB'* package
563 (94).
564
565 *The effect of copper on the distribution of siderophore production*
566 To demonstrate that copper selectively favored intermediate siderophore levels, we
567 determined the effect size of copper for bacterial taxa that commonly occurred in both
568 copper treatments and related this to their mean siderophore production under non-polluted
569 conditions, using a Spearman rank correlation. Effect size was calculated using the
570 *'cohen.d'* function in the *'effsize'* package (95). Cohen's *d* takes the difference between
571 two means and expresses it in standard deviation units, with negative values indicating a
572 reduction in siderophore levels in response to copper, and *vice versa* for positive values.
573
574 *Effect-size in compost communities evolved with SBW25*
575 To determine the impact of copper on the siderophore production of both SBW25 and
576 community isolates that had evolved together, we used a hierarchical Bayesian linear
577 model which accounts for the differing variances associated with explanatory variables
578 (i.e. siderophore measurements from community isolates were taken from diverse bacterial
579 strains even within a single replicate community, as opposed to the originally isogenic
580 SBW25 stocks):

581 $$y_i \sim N(\mu_i, \sigma_{group[i]})$$

582 $$\mu_i = \lambda_{group[i],replicate[i]}$$

583 $$\lambda_{j,k} \sim N(\nu_j, \tau_j) \text{ , for } j = 1..4,\ k = 1..6$$

584 $$\nu_j = \alpha_{X1[j]} + \beta_{X1[j]}X2_j \text{ , for } j = 1..4$$

585 $$\alpha_j \sim N^{+}(0,1) \text{ , for } j = 1..2$$

586 $$\beta_j \sim N(0,0.25) \text{ , for } j = 1..2$$

587 $$\sigma_j \sim \text{Exponential}(0.2) \text{ , for } j = 1..4$$

588 $$\tau_j \sim \text{Exponential}(0.2)\text{ , for } j = 1..4$$

589 where X1 is a vector of indices indicating SBW25 vs community samples; X2 is a vector
590 indicator indicating the presence/absence of copper; *replicate* and *group* are vectors of
591 indices denoting the replicate microcosm (from a given group) and the combination of
592 isolate type (SBW25 vs community) and presence/absence of copper for each data point.
593 The model above, with separate standard deviation terms (σ) for each group was chosen
594 over models with one or two (determined by isolate type or copper presence) standard
595 deviation terms after model selection by Pareto smoothed importance sampling leave one
596 out (PSIS-LOO) cross validation (96). Inference was performed by Markov chain Monte
597 Carlo using Turing.jl (97) in the Julia programming language (98): 4 chains of 1000
598 samples each using the No U-Turn Sampler (NUTS) algorithm (99), with all R-hat scores
599 < 1.01. 95% credible intervals were calculated as the 95% highest posterior density interval
600 (HPDI) using StatisticalRethinking.jl
601 (https://github.com/StatisticalRethinkingJulia/StatisticalRethinking.jl). Subsequently, point
602 estimates were obtained by computing the *maximum a posteriori* parameter estimates of
603 the same model, using Optim.jl (100) in conjunction with Turing.jl. To compare the
604 positive affect of copper on siderophore production amongst compost community isolates
605 with the negative affect on SBW25, we computed the posterior distribution of the
606 combined effect as $\beta_1 + \beta_2$ by element-wise addition of Markov chain samples. The same
607 approach was used to infer the posterior distribution of the difference between community
608 and SBW25 siderophore production with copper ($\alpha_2 - \alpha_1$) and without ($\alpha_2 + \beta_2 - (\alpha_1 + \beta_1)$).
609

610 *The role of direct and indirect selection in favoring intermediate siderophore levels*
611 To test for whether copper-adapted clones of SBW25 evolved greater resistance to copper
612 than those evolved under unpolluted conditions, we used a LMM model on *m* with
613 evolutionary background as fixed explanatory variable. To account for non-independency

614 of observations, we fitted random intercepts for individual microcosms. However, the
615 variation explained by the random intercepts approached zero, causing singularity issues
616 when fitting the LMM using the '*lme4'* package. We therefore used the default setting of
617 the nonlinear optimizer in the *'glmmTMB'* function for parameter estimation. We next
618 tested whether increased investment in siderophores conferred greater copper tolerance by
619 including siderophore production in the evolutionary LMM described above.

620 We determined whether siderophores were selectively favored when iron was
621 needed for growth by propagating a pyoverdine-producing and pyoverdine-deficient
622 mutant strain of SBW25 in isolation and together at different inoculation densities under
623 copper-polluted and unpolluted conditions. We first determined whether pyoverdines
624 provide an *absolute* growth benefit to the wild-type producer under toxic copper conditions
625 by comparing the Malthusian parameter ($m$) of individually grown strains using a GLM
626 with density × strain × copper as explanatory variables, as well as all possible 2- and 3-way
627 interactions. We next determined whether density differentially affected the performance
628 of the pyoverdine producing and non-producing strains during direct competition, using a
629 LMM with $m$ as response variable and strain × frequency as explanatory variables and
630 random intercepts fitted for each microcosm ($n$ = 24) to account for non-independency of
631 paired observations within microcosms. Finally, we were interested in how density
632 affected the relative fitness of the pyoverdine-producing strain ($r_{producer}$ =
633 $m_{producer}/m_{non-producer}$) (84) during direct competition with the mutant as a function of
634 copper stress. We expected the pyoverdine-producing strain to be at a selective
635 disadvantage under low growth conditions (i.e. when iron is not limiting growth). We
636 tested this using a GLM with $r_{producer}$ as response variable and copper × density as
637 explanatory variables, as well as their 2-way interaction.

638 Finally, we determined whether social exploitation could have played an additional
639 role in selecting against high siderophore levels in response to copper stress. To this end,

640 we competed the pyoverdine-producing wildtype strain SBW25 and a pyoverdine-deficient
641 mutant at a low (1%) or high (99%) frequency in copper-polluted and unpolluted compost.
642 We determined whether copper differentially affected the relative fitness of the
643 pyoverdine-deficient mutant ($s_{mutant} = m_{mutant} - m_{wild-type}$) (84) as a function of its
644 initial frequency. Note that we used the selection rate ($s$) as a measure of relative fitness as
645 some of the Malthusian growth parameters were negative (SI Appendix, Fig. S7). We
646 expected the pyoverdine-deficient mutant to reap greater fitness benefits when rare and
647 tested this hypothesis using a GLM with $s_{mutant}$ as response variable and initial frequency
648 (low or high) × copper as fixed explanatory variables, as well as their interaction.
649

650 **Acknowledgments |** We thank the three anonymous reviewers for their valuable
651 comments and Daniel Padfield for advice on statistical analyses. This work was funded by
652 AXA Research Fund, Biotechnology and Biological Sciences Research Council (BBSRC:
653 BB/K00324) and Natural Environment Research Council (NERC: NE/V012347/1) grants
654 awarded to AB and a UK Research Innovation (UKRI) Future Leader Fellowship (UKRI-
655 FLF: MR/V022482/1) awarded to EH. SOB was funded by a 'Bridging the Gaps' award
656 and PhD scholarship from the University of Exeter. AML was supported by FP7 Marie
657 Skłodowska-Curie International Incoming Fellowship (IIF) (no. 331163).
658

659 **Author Contributions |** EH, AML, SOB, DJH, AB conceived and designed the study. EH,
660 AML, SOB, TM, JSP, FB collected the data. EH, AN and FB carried out data analyses.
661 EH, AB wrote the first draft of the manuscript, and all authors contributed to revisions.
662

663 **Competing Interest Statement |** The authors declare no competing interests.
664

**Open Access |** For the purpose of open access, the authors have applied a Creative Commons Attribution (CC BY) license to any Author Accepted Manuscript version arising from this submission'.

## References


1. T. G. Barraclough, How do species interactions affect evolutionary dynamics across whole communities? *Annu. Rev. Ecol. Evol. Syst.* **46**, 25-48 (2015).
2. J. Cairns, R. Jokela, L. Becks, V. Mustonen, T. Hiltunen, Repeatable ecological dynamics govern response of experimental community to antibiotic pulse perturbation. *Nat. Ecol. Evol.* **4**, 1385-1394 (2020).
3. R. Evans *et al.*, Eco-evolutionary dynamics set the tempo and trajectory of metabolic evolution in multispecies communities. *Curr. Biol.* **30**, 4984-4988 (2020).
4. A. B. Chase, C. Weihe, J. B. Martiny, Adaptive differentiation and rapid evolution of a soil bacterium along a climate gradient. *PNAS* **118**, e2101254118 (2021).
5. F. Fiegna, A. Moreno-Letelier, T. Bell, T. G. Barraclough, Evolution of species interactions determines microbial community productivity in new environments. *ISME* **9**, 1235-1245 (2015).
6. N. G. Hairston Jr, S. P. Ellner, M. A. Geber, T. Yoshida, J. A. Fox, Rapid evolution and the convergence of ecological and evolutionary time. *Ecol. Lett.* **8**, 1114-1127 (2005).
7. F. A. Gorter, M. Manhart, M. Ackermann, Understanding the evolution of interspecies interactions in microbial communities. *Philos. Trans. R. Soc. Lond. B Biol. Sci.* **375**, 20190256 (2020).
8. J. B. Martiny *et al.*, Investigating the eco‐evolutionary response of microbiomes to environmental change. *Ecol. Lett.* **26**, S81-S90 (2023).
9. M. Lässig, V. Mustonen, A. M. Walczak, Predicting evolution. *Nat. Ecol. Evol.* **1**, 1-9 (2017).

692 10. N. Meroz, N. Tovi, Y. Sorokin, J. Friedman, Community composition of microbial
693 microcosms follows simple assembly rules at evolutionary timescales. *Nat.*
694 *Commun.* **12**, 1-9 (2021).
695 11. Y. Yang, Emerging patterns of microbial functional traits. *Trends Microbiol.* **29**,
696 874-882 (2021).
697 12. M. Cavaliere, S. Feng, O. S. Soyer, J. I. Jiménez, Cooperation in microbial
698 communities and their biotechnological applications. *Environ. Microbiol.* **19**, 2949-
699 2963 (2017).
700 13. S. Shibasaki, S. Mitri, Controlling evolutionary dynamics to optimize microbial
701 bioremediation. *Evol. Appl.* **13**, 2460-2471 (2020).
702 14. A. N. Yadav *et al.*, Beneficial microbiomes: biodiversity and potential
703 biotechnological applications for sustainable agriculture and human health. *J. appl.*
704 *biol.* **5**, 4-7 (2017).
705 15. T. Scheuerl *et al.*, Bacterial adaptation is constrained in complex communities. *Nat.*
706 *Commun.* **11**, 1-8 (2020).
707 16. M. Castledine, D. Padfield, A. Buckling, Experimental (co) evolution in a multi‐
708 species microbial community results in local maladaptation. *Ecol. Lett.* **23**, 1673-
709 1681 (2020).
710 17. D. Lawrence *et al.*, Species interactions alter evolutionary responses to a novel
711 environment. *PLoS Biol.* **10**, e1001330 (2012).
712 18. A. Buckling, R. Craig Maclean, M. A. Brockhurst, N. Colegrave, The Beagle in a
713 bottle. *Nature* **457**, 824-829 (2009).
714 19. C. De Mazancourt, E. Johnson, T. Barraclough, Biodiversity inhibits species'
715 evolutionary responses to changing environments. *Ecol. Lett.* **11**, 380-388 (2008).
716 20. P. Gómez, A. Buckling, Real-time microbial adaptive diversification in soil. *Ecol.*
717 *Lett.* **16**, 650-655 (2013).

718 21. M. A. Brockhurst, N. Colegrave, D. J. Hodgson, A. Buckling, Niche occupation
719 limits adaptive radiation in experimental microcosms. *PLoS One* **2**, e193 (2007).
720 22. R. S. Etienne, B. Haegeman, A conceptual and statistical framework for adaptive
721 radiations with a key role for diversity dependence. *Am. Nat.* **180**, E75-E89 (2012).
722 23. A. Jousset, N. Eisenhauer, M. Merker, N. Mouquet, S. Scheu, High functional
723 diversity stimulates diversification in experimental microbial communities. *Sci.*
724 *Adv.* **2**, e1600124 (2016).
725 24. D. I. Bolnick *et al.*, Why intraspecific trait variation matters in community ecology.
726 *TREE* **26**, 183-192 (2011).
727 25. R. Lanfear, H. Kokko, A. Eyre-Walker, Population size and the rate of evolution.
728 *TREE* **29**, 33-41 (2014).
729 26. J. Johansson, Evolutionary responses to environmental changes: how does
730 competition affect adaptation? *Evolution* **62**, 421-435 (2008).
731 27. R. Kummerli, K. T. Schiessl, K. McNeill, M. Ackermann, Habitat structure and the
732 evolution of diffusible siderophores in bacteria. *Ecol. Lett.* **17**, 1536-1655 (2014).
733 28. R. C. Hider, X. Kong, Chemistry and biology of siderophores. *Nat. Prod. Rep.* **27**,
734 637-657 (2010).
735 29. C. Ratledge, L. G. Dover, Iron metabolism in pathogenic bacteria. *Annu. Rev.*
736 *Microbiol.* **54**, 881-941 (2000).
737 30. I. J. Schalk, M. Hannauer, A. Braud, New roles for bacterial siderophores in metal
738 transport and tolerance. *Environ. Microbiol.* **13**, 2844-2854 (2011).
739 31. A. Braud, V. Geoffroy, F. Hoegy, G. L. A. Mislin, I. J. Schalk, Presence of the
740 siderophores pyoverdine and pyochelin in the extracellular medium reduces toxic
741 metal accumulation in *Pseudomonas auruginosa* and increases bacterial metal
742 tolerance. *Environ. Microbiol. Rep.* **2**, 419-425 (2010).

743 32. S. O'Brien *et al.*, No effect of intraspecific relatedness on public goods cooperation
744 in a complex community. *Evolution* **72**, 1165-1173 (2018).
745 33. E. Hesse *et al.*, Ecological selection of siderophore-producing microbial taxa in
746 response to heavy metal contamination. *Ecol. Lett.* **21**, 117-127 (2018).
747 34. E. Hesse *et al.*, Stress causes interspecific facilitation within a compost community.
748 *Ecol. Lett.* **24**, 2169-2177 (2021).
749 35. J. Kramer, Ö. Özkaya, R. Kümmerli, Bacterial siderophores in community and host
750 interactions. *Nat. Rev. Microbiol.*, 1-12 (2020).
751 36. E. Hesse *et al.*, Anthropogenic remediation of heavy metals selects against natural
752 microbial remediation. *Proc B* **286**, 20190804 (2019).
753 37. P. B. Rainey, M. J. Bailey, Physical and genetic map of the Pseudomonas
754 fluorescens SBW25 chromosome. *Molecular Microbiology* **19**, 521-533 (1996).
755 38. A. M. Lujan, P. Gomez, A. Buckling, Siderophore cooperation of the bacterium
756 *Pseudomonas fluorescens* in soil. *Biol. Lett.* **11**, 20140934 (2015).
757 39. C. D. Moon *et al.*, Genomic, genetic and structural analysis of pyoverdine-
758 mediated iron acquisition in the plant growth-promoting bacterium *Pseudomonas*
759 *fluorescens* SBW25. *BMC Microbiol.* **8**, 7 (2008).
760 40. N. Jiricny *et al.*, Fitness correlates with the extent of cheating in a bacterium. *J.*
761 *Evol. Biol.* **23**, 738-747 (2010).
762 41. A. S. Griffin, S. A. West, A. Buckling, Cooperation and competition in pathogenic
763 bacteria. *Nature* **430**, 1024-1027 (2004).
764 42. S. Pollak *et al.*, Public good exploitation in natural bacterioplankton communities.
765 *Sci. Adv.* **7**, eabi4717 (2021).
766 43. J. Kramer, Ö. Özkaya, R. Kümmerli, Bacterial siderophores in community and host
767 interactions. *Nat. Rev. Microbiol.* **18**, 152-163 (2020).

768 44. J. Galet *et al.*, *Pseudomonas fluorescens* pirates both ferrioxamine and
769 ferricoelichelin siderophores from *Streptomyces ambofaciens*. *Appl. Environ.*
770 *Microbiol.* **81**, 3132-3141 (2015).
771 45. P. Cornelis, S. Matthijs, Diversity of siderophore-mediated iron uptake systems in
772 fluorescent pseudomonads: not only pyoverdines. *Environ. Microbiol.* **4**, 787-798
773 (2002).
774 46. R. Niehus, A. Picot, N. M. Oliveira, S. Mitri, K. R. Foster, The evolution of
775 siderophore production as a competitive trait. *Evolution* **71**, 1443-1455 (2017).
776 47. A. R. Figueiredo, Ö. Özkaya, R. Kümmerli, J. Kramer, Siderophores drive invasion
777 dynamics in bacterial communities through their dual role as public good versus
778 public bad. *Ecol. Lett.* **25**, 138-150 (2022).
779 48. J. D. Palmer, K. R. Foster, Bacterial species rarely work together. *Science* **376**,
780 581-582 (2022).
781 49. J. J. Morris, R. E. Lenski, E. R. Zinser, The Black Queen hypothesis: evolution of
782 dependencies through adaptive gene loss. *MBio* **3**, 2 e00036-00012 (2012).
783 50. W. D. Hamilton, The genetical evolution of social baviour. I. *J. Theor. Biol.* **7**, 1-16
784 (1964).
785 51. L. J. Belcher, A. E. Dewar, M. Ghoul, S. A. West, Kin selection for cooperation in
786 natural bacterial populations. *PNAS* **119**, e2119070119 (2022).
787 52. M. Garcia-Garcera, E. P. Rocha, Community diversity and habitat structure shape
788 the repertoire of extracellular proteins in bacteria. *Nat. Commun.* **11**, 1-11 (2020).
789 53. O. X. Cordero, L.-A. Ventouras, E. F. DeLong, M. F. Polz, Public good dynamics
790 drive evolution of iron acquisition strategies in natural bacterioplankton
791 populations. *PNAS* **109**, 20059-20064 (2012).
792 54. S. A. West, A. S. Griffin, A. Gardner, S. P. Diggle, Social evolution theory for
793 microorganisms. *Nat. Rev. Microbiol.* **4**, 597-608 (2006).

794 55. S. A. West, S. P. Diggle, A. Buckling, A. Gardner, A. S. Griffin, The social lives of
795 microbes. *Annu. Rev. Ecol. Syst.* **38**, 53-77 (2007).
796 56. B. J. Crespi, The evolution of social behavior in microorganisms. *TREE* **16**, 178-
797 183 (2001).
798 57. J. Gore, H. Youk, A. Van Oudenaarden, Snowdrift game dynamics and facultative
799 cheating in yeast. *Nature* **459**, 253-256 (2009).
800 58. G. Hardin, The tragedy of the commons. *Science* **162**, 1243-1248 (1968).
801 59. R. Axelrod, W. D. Hamilton, The evolution of cooperation. *Science* **211**, 1390-
802 1396 (1981).
803 60. J. L. Sachs, U. G. Mueller, T. P. Wilcox, J. J. Bull, The evolution of cooperation.
804 *Q. Rev. Biol.* **79**, 135-160 (2004).
805 61. H. H. Lee, M. N. Molla, C. R. Cantor, J. J. Collins, Bacterial charity work leads to
806 population-wide resistance. *Nature* **467**, 82-85 (2010).
807 62. I. Frost *et al.*, Cooperation, competition and antibiotic resistance in bacterial
808 colonies. *ISME* **12**, 1582-1593 (2018).
809 63. C. D. Nadell, J. B. Xavier, K. R. Foster, The sociobiology of biofilms. *FEMS*
810 *Microbiol. Rev.* **33**, 206-224 (2008).
811 64. K. P. Rumbaugh *et al.*, Quorum sensing and the social evolution of bacterial
812 virulence. *Curr. Biol.* **19**, 341-345 (2009).
813 65. I. Eleftherianos *et al.*, An antibiotic produced by an insect-pathogenic bacterium
814 suppresses host defenses through phenoloxidase inhibition. *PNAS* **104**, 2419-2424
815 (2007).
816 66. B. Raymond, S. A. West, A. S. Griffin, M. B. Bonsall, The dynamics of
817 cooperative bacterial virulence in the field. *Science* **337**, 85-88 (2012).

818 67. T. Köhler, G. G. Perron, A. Buckling, C. Van Delden, Quorum sensing inhibition
819 selects for virulence and cooperation in *Pseudomonas aeruginosa*. *PLoS Pathog.* **6**,
820 e1000883 (2010).
821 68. P. Gómez *et al.*, Local adaptation of a bacterium is as important as its presence in
822 structuring a natural microbial community. *Nat. Commun.* **7**, 12453 (2016).
823 69. R. Kummerli, A. S. Griffin, S. A. West, A. Buckling, F. Harrison, Viscous medium
824 promotes cooperation in the pathogenic bacterium *Pseudomonas aeruginosa*. *Proc*
825 *B* **276**, 3531-3538 (2009).
826 70. E. Butaitė, M. Baumgartner, S. Wyder, R. Kümmerli, Siderophore cheating and
827 cheating resistance shape competition for iron in soil and freshwater Pseudomonas
828 communities. *Nat. Commun.* **8**, 414 (2017).
829 71. A. Ross-Gillespie, A. Gardner, S. A. West, A. S. Griffin, Frequency dependence
830 and cooperation: theory and a test with bacteria. *Am. Nat.* **170**, 331-342 (2007).
831 72. H. Heuer, K. Smalla, Plasmids foster diversification and adaptation of bacterial
832 populations in soil. *FEMS Microbiol. Rev.* **36**, 1083-1104 (2012).
833 73. T. Robinson, P. Smith, E. R. Alberts, M. Colussi-Pelaez, M. Schuster, Cooperation
834 and cheating through a secreted aminopeptidase in the *Pseudomonas aeruginosa*
835 RpoS response. *Mbio* **11**, 10.1128/mbio. 03090-03019 (2020).
836 74. A. Dragoš *et al.*, Evolution of exploitative interactions during diversification in
837 Bacillus subtilis biofilms. *FEMS Microbiol. Ecol.* **94**, fix155 (2018).
838 75. S. O'Brien, D. J. Hodgson, A. Buckling, Social evolution of toxic metal
839 bioremediation in *Pseudomonas aeruginosa*. *Proc B* **281**, 20140858 (2014).
840 76. A. K. Hottes *et al.*, Bacterial adaptation through loss of function. *PLoS genetics* **9**,
841 e1003617 (2013).
842 77. T. Dimitriu *et al.*, Genetic information transfer promotes cooperation in bacteria.
843 *PNAS* **111**, 11103-11108 (2014).

844 78. D. J. Rankin, E. P. Rocha, S. P. Brown, What traits are carried on mobile genetic
845 elements, and why? *Heredity (Edinb.)* **106**, 1-10 (2011).
846 79. A. E. Dewar, L. J. Belcher, T. W. Scott, S. A. West, Genes for cooperation are not
847 more likely to be carried by plasmids. *Proc B* **291**, 20232549 (2024).
848 80. T. Nogueira *et al.*, Horizontal gene transfer of the secretome drives the evolution of
849 bacterial cooperation and virulence. *Curr. Biol.* **19**, 1683-1691 (2009).
850 81. O. X. Cordero, P. Hogeweg, The impact of long-distance horizontal gene transfer
851 on prokaryotic genome size. *Proceedings of the National Academy of Sciences* **106**,
852 21748-21753 (2009).
853 82. X. Cheng, I. de Bruijn, M. van der Voort, J. E. Loper, J. M. Raaijmakers, The Gac
854 regulon of *Pseudomonas fluorescen*s SBW25. *Environ. Microbiol. Rep.* **5**, 608-619
855 (2013).
856 83. B. Schwyn, J. B. Neilands, Universal chemical assay for the detection and
857 determination of siderophores. *Anal. Biochem.* **160**, 47-56 (1987).
858 84. R. E. Lenski, M. R. Rose, S. C. Simpson, S. C. Tadler, Long-term experimental
859 evolution in *Escherichia coli*. I. Adaptation and divergence during 2000
860 generations. *Am. Nat.* **138**, 1315-1341 (1991).
861 85. B. J. Callahan *et al.*, DADA2: high-resolution sample inference from Illumina
862 amplicon data. *Nat. Methods* **13**, 581-583 (2016).
863 86. M. Kearse *et al.*, Geneious Basic: an integrated and extendable desktop software
864 platform for the organization and analysis of sequence data. *Bioinformatics* **28**,
865 1647-1649 (2012).
866 87. P. D. Schloss *et al.*, Introducing Mothur: open-source, platform-independent,
867 community-supported software for describing and comparing microbial
868 communities. *Appl. Environ. Microbiol.* **75**, 7537-7541 (2009).

88. R. V. Lenth, Least-squares means: the R package lsmeans. *J. Stat. Softw.* **69**, 1-33 (2016).

89. F. Hartig (2020) DHARMa: Residual diagnostics for hierachical (multi-level / mixed) regression models. R package version 0.3.3.0.

90. H. Wickham, *ggplot2: Elegant Graphics for Data Analysis* (Springer Verlag, New York, 2016).

91. D. Bates, M. Maechler, B. Bolker, S. Walker, Fitting Linear Mixed-Effects Models Using lme4. *J. Stat. Softw.* **67**, 1-48 (2015).

92. J. Oksanen *et al.* (2010) vegan: Community Ecology Package. R package version 2.5-4.

93. M. I. Love, W. Huber, S. Anders, Moderated estimation of fold change and dispersion for RNA-seq data with DESeq2. *Genome Biol.* **15**, 550 (2014).

94. M. E. Brooks *et al.*, glmmTMB balances speed and flexibility among packages for zero-inflated generalized linear mixed modelling. *The R Journal* **9**, 378-400 (2017).

95. M. Torchiano (2016) Effsize - A package for efficient effect size computation

96. A. Vehtari, A. Gelman, J. Gabry, Practical Bayesian model evaluation using leave-one-out cross-validation and WAIC. *Stat. Comput.* **27**, 1413-1432 (2017).

97. H. Ge, K. Xu, Z. Ghahramani (2018) Turing: a language for flexible probabilistic inference. in *International conference on artificial intelligence and statistics* (PMLR), pp 1682-1690.

98. J. Bezanson, A. Edelman, S. Karpinski, V. B. Shah, Julia: A fresh approach to numerical computing. *SIAM review* **59**, 65-98 (2017).

99. M. D. Hoffman, A. Gelman, The No-U-Turn sampler: adaptively setting path lengths in Hamiltonian Monte Carlo. *J. Mach. Learn. Res.* **15**, 1593-1623 (2014).

100. P. K. Mogensen, A. N. Riseth, Optim: A mathematical optimization package for Julia. *JOSS* **3** (2018).

895 ## Figure legends

896 **Figure 1 | Copper favors siderophore-producing taxa within the compost community.**
897 Panel **(A)** shows that copper-polluted (copper [+], orange) communities (*n* =6) produced on
898 average larger amounts of siderophore compared to copper-free (copper [-], blue)
899 communities following six weeks of evolution in isolation (light shading) or in co-culture
900 with SBW25 (dark shading) (*n* = 6 communities per treatment). Brown line and shaded
901 area depict mean ± SE siderophore production of the ancestral communities (*n* = 12) prior
902 to copper amendment. Boxes depict upper and lower quartiles of treatment-specific raw
903 data with the center line showing the median and whiskers providing a measure of 1.5x
904 interquartile range. Points represent the mean value per community based on twenty-four
905 isolates, with within-community variance indicated by different point sizes. Note that for
906 some replicate communities we isolated < 24 isolates, yielding a total sample size of *n* =
907 548. Panel **(B)** depicts a Principal Coordinate Analysis (PCoA) plot based on Bray-Curtis
908 dissimilarities between compost communities (excluding SWB25). The percentage of
909 variation explained is shown on each axis, calculated from the relevant eigenvalues.
910 Communities belonging to the same treatment are joined with straight colored lines
911 ($control_{no\ SBW25}$ = light blue, $control_{SBW25}$ = dark blue, $copper_{no\ SBW25}$ = orange,
912 $copper_{SBW25}$= red), with large points representing treatment-specific centroids and small
913 points individual microcosms. Dissimilarities were calculated using data on the total
914 abundance of different isolates (identified at genus level) within each community that were
915 assayed for siderophore production (*n* = 24 per community). Panel (**C**) depicts the effect of
916 coper on the abundance of bacterial taxa in the compost community. The log2-fold change
917 in total abundance of the ten most common genera when comparing communities that had
918 evolved in unpolluted versus copper-polluted compost. Of the taxa tested, three
919 significantly differed in terms of total abundance between copper-free versus copper-

920 polluted treatments: while *Cupviavidus* was positively affected*, Achromobacter and*
921 *Lysinibacillus* were both negatively affected by copper stress (see SI Appendix, Table S1
922 table for Wald test and P-values). Points represent estimated log2-fold change in total
923 abundance of each taxon in response to copper-stress (averaged across culturing
924 conditions) ± standard error bars. Genera are color-coded based on their mean across-
925 treatment siderophore production, ranging from relatively low (blue) to intermediate
926 (orange) and high (red) siderophore production. Panel **(D)** depicts the relative abundance of
927 the ten most common culturable compost taxa, excluding SWB25, following six weeks of
928 evolution under different selection regimes. Genera are listed in order of their across-
929 treatment mean siderophore production, increasing from top to bottom, such that orange-
930 coral taxa produce relatively intermediate to high levels of siderophores.
931
932 **Figure 2 | Toxic copper favors the evolution of reduced siderophore production within**
933 **SBW25**. Boxplot showing that copper (copper [+], brown) selected for lower mean
934 siderophore levels in SBW25 populations compared to copper-free conditions (copper [-],
935 pink) irrespective of whether populations evolved in isolation (light-shading) or in co-
936 culture with the compost community (dark-shading) ($n$ = 6 populations per treatment).
937 Orange line and shaded area depict mean ± SE siderophore production of ancestral SBW25
938 populations ($n$ = 12) prior to copper amendment. Boxes depict the upper and lower
939 quartiles of treatment-specific raw data with the center line showing the median and
940 whiskers providing a measure of 1.5x interquartile range. Points represent the mean value
941 per population ($n$ =6 per copper treatment) based on twenty-four clones where possible,
942 with within-population variance given by different point sizes. Note that for some replicate
943 communities we isolated < 24 clones, yielding a total sample size of $n$ = 501.
944

945 **Figure 3 | Copper leads to trait convergence by selecting against siderophore extremes.**
946 Panel **(A)** shows the frequency distributions of siderophore production in ancestral SBW25
947 populations (blue) and compost communities (brown) prior to copper amendment.
948 Siderophore data were pooled across copper treatments and replicates ($n$ = 24 isolates for
949 each of the twelve replicate SBW25 populations / compost communities). Panel **(B)**
950 demonstrates that the distribution of siderophore production in SBW25 (blue) and the
951 community (brown) converges in response to copper stress, independent of whether these
952 evolved in isolation (top panel) or in co-culture (bottom panel). Siderophore data were
953 pooled across replicates ($n$ = 24 isolates for replicate population/community). Note that for
954 some replicates we isolated < 24 clones/isolates of SBW25 or the community, yielding a
955 total sample size of $n$ = 1049. Brown and blue vertical lines depict mean siderophore
956 production of the ancestral compost communities and SBW25 populations, respectively.
957
958 **Figure 4 | Benefit of different siderophore strategies is context dependent.** Boxplot
959 showing **(A)** the Malthusian growth parameter ($m$) of the pyoverdine-deficient mutant
960 (blue) and pyoverdine-producing wild-type SBW25 strain (gold) as a function of
961 inoculation density when individually grown in copper-polluted (copper [+]) and
962 unpolluted (copper [-]) compost **(B)** the pyoverdine-deficient 'cheat' receiving a relative
963 selective benefit ($S_{mutants}$ > 0) when rare, in particular when competing with the wild-
964 type producer in copper-polluted compost. Strains were co-inoculated together at different
965 frequencies (1% or 99%) in copper-polluted (copper [+]) and unpolluted (copper [-])
966 compost. Blue horizontal line depicts equal fitness ($S_{mutants}$ = 0) of competing strains.
967 Boxes depict the upper and lower quartiles of treatment-specific raw data with the center
968 line showing the median and whiskers providing a measure of 1.5x interquartile range, and
969 points show the raw data for each replicate population.

970 **Figure 1**

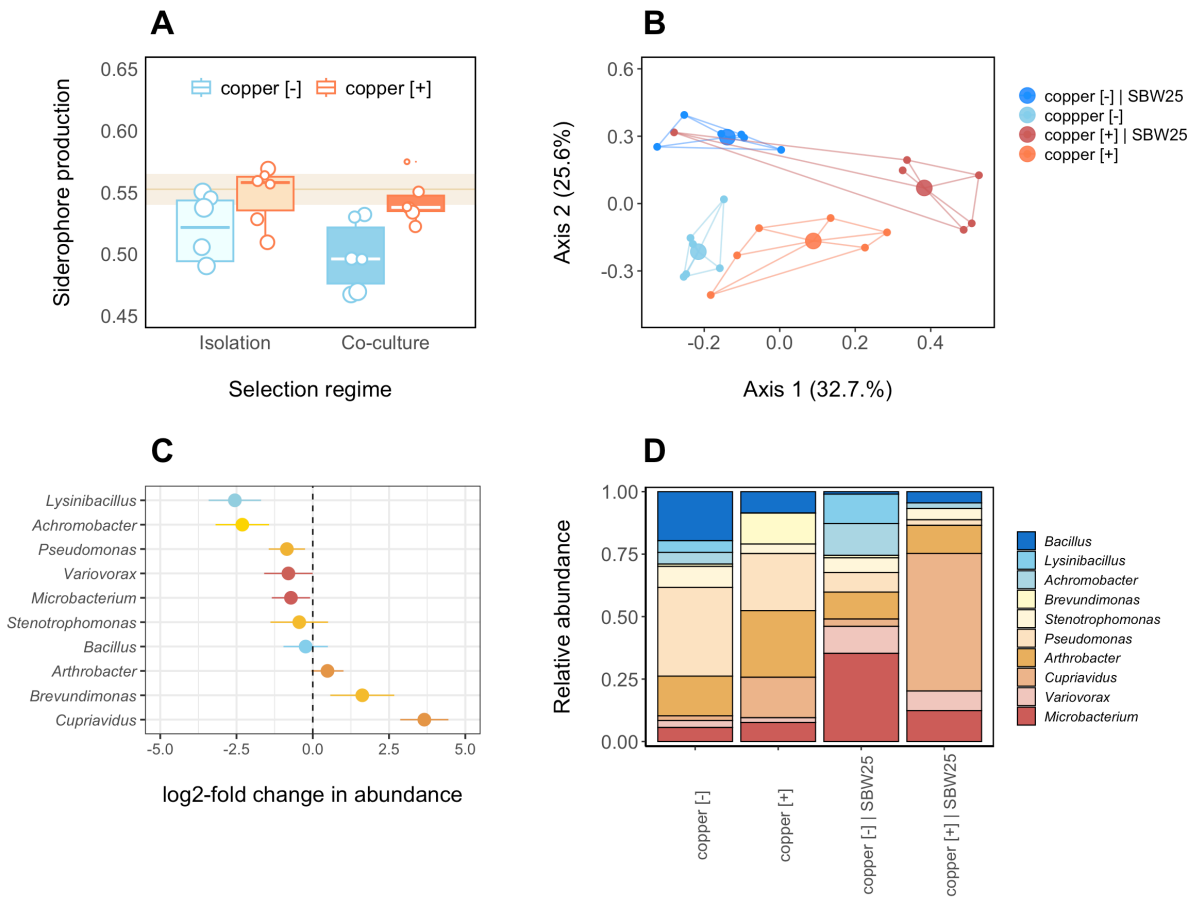
A
Siderophore production
0.65
0.60
0.55
0.50
0.45
copper [-]
copper [+]
Isolation
Co-culture
Selection regime
B
Axis 2 (25.6%)
0.6
0.3
0.0
-0.3
-0.2
0.0
0.2
0.4
Axis 1 (32.7.%)
copper [-] | SBW25
coppper [-]
copper [+] | SBW25
copper [+]
C
Lysinibacillus
Achromobacter
Pseudomonas
Variovorax
Microbacterium
Stenotrophomonas
Bacillus
Arthrobacter
Brevundimonas
Cupriavidus
-5.0
-2.5
0.0
2.5
5.0
log2-fold change in abundance
D
Relative abundance
1.00
0.75
0.50
0.25
0.00
copper [-]
copper [+]
copper [-] | SBW25
copper [+] | SBW25
Bacillus
Lysinibacillus
Achromobacter
Brevundimonas
Stenotrophomonas
Pseudomonas
Arthrobacter
Cupriavidus
Variovorax
Microbacterium

971 **Figure 2**

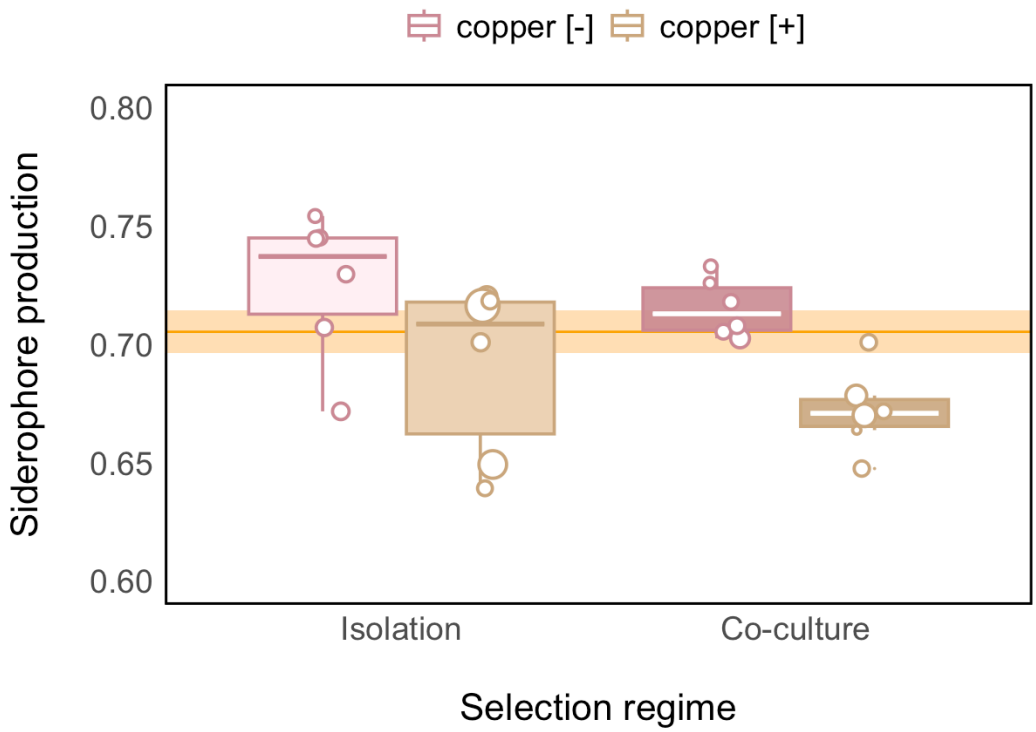
copper [-]
copper [+]
Siderophore production
0.80
0.75
0.70
0.65
0.60
Isolation
Co-culture
Selection regime

972 **Figure 3**

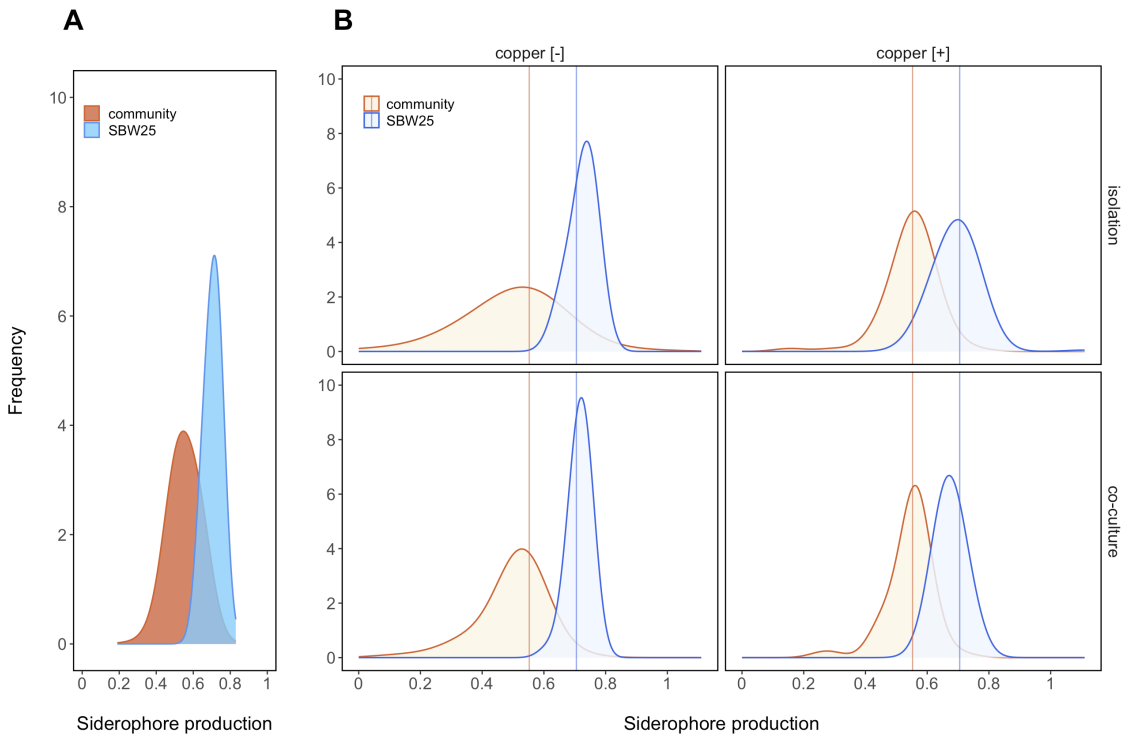
A
B
community
SBW25
Frequency
Siderophore production
copper [-]
copper [+]
isolation
co-culture
0
2
4
6
8
10
0.2
0.4
0.6
0.8
1

973 **Figure 4**

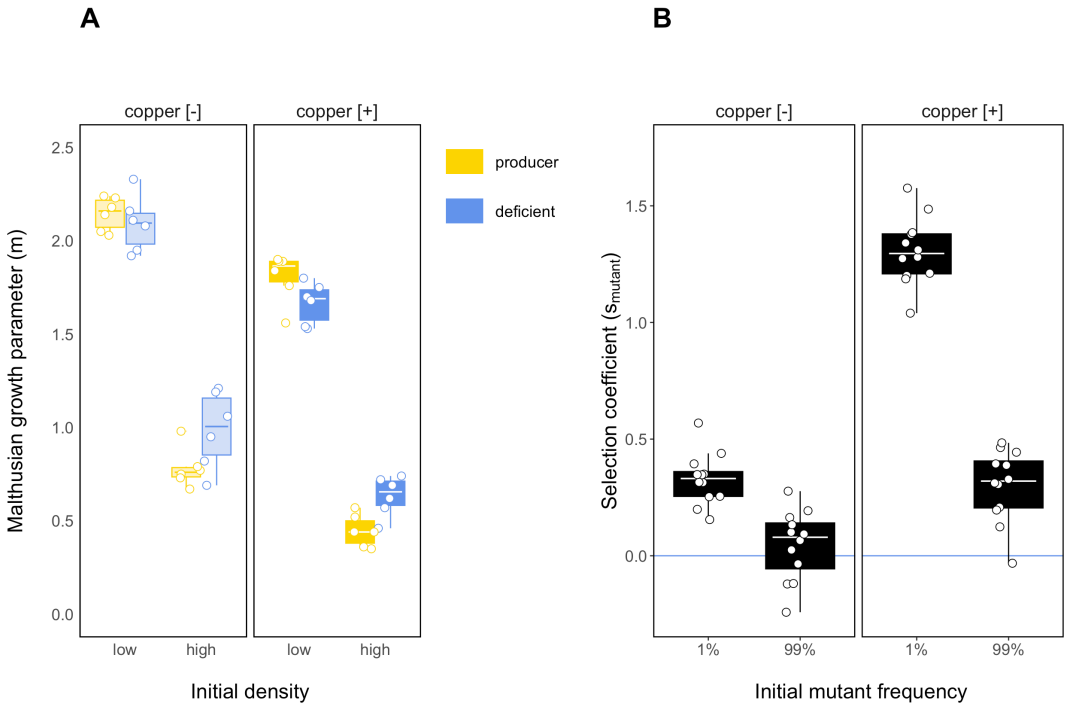
A
B
copper [-]
copper [+]
Malthusian growth parameter (m)
2.5
2.0
1.5
1.0
0.5
0.0
low
high
Initial density
producer
deficient
Selection coefficient ($s_{mutant}$)
1.5
1.0
0.5
0.0
1%
99%
Initial mutant frequency